Journal of the Arkansas Academy of Science

Volume 71 Article 31

2017

Restrained Shrinkage of Fly Ash Based Geopolymer Concrete and Analysis of Long Term Shrinkage Prediction Models

Md R. Islam
Southern Arkansas University, mdislam@saumag.edu

Mahbub K. Ahmed
southern arkansas university, mahbubahmed@saumag.edu

Hosney Ara Begum
Bangladesh Council of Science and Industrial Research, hosneyara@gmail.com

Erez N. Allouche
Louisiana Tech University, allouche@latech.edu

Restrained Shrinkage of Fly Ash Based Geopolymer Concrete and Analysis of Long Term Shrinkage Prediction Models

Cover Page Footnote
The author would like to thank Trenchless Technology Center of Louisiana Tech University for the use of its facilities. Special thanks to Dr. Carlos Montes for his suggestions and help to access the material characterization lab of the micro-manufacturing institute of Louisiana Tech University.

Restrained Shrinkage of Fly Ash Based Geopolymer Concrete and Analysis of Long Term Shrinkage Prediction Models

M.R. Islam*, M.K. Ahmed, H.A. Begum, and E.N. Allouche

Department of Engineering and Physics, Southern Arkansas University, Magnolia, AR 71753

*Correspondence: mdislam@saumag.edu

Running Title: Restrained Shrinkage of Geopolymer Concrete and Shrinkage Prediction Model for GPC

Abstract

The research presented in this manuscript describes the procedure to quantify the restrained shrinkage of geopolymer concrete (GPC) using ring specimen. Massive concrete structures are susceptible to shrinkage and thermal cracking. This cracking can increase the concrete permeability and decrease the strength and design life. This test is comprised of evaluating geopolymer concrete of six different mix designs including different activator solution to fly ash ratio subjected to both restrained and free shrinkage. Test results obtained from this experimental setup were plotted along with the available empirical equation to observe the shrinkage strain of GPC and a model was suggested to predict the shrinkage strain of GPC. It was found from this study that along with activator solution to fly ash ratio the final compressive strength of GPC plays an important role on shrinkage strain.

Introduction

In high strength concrete structure and concrete repair, overlay, long span slab, differential drying through the thickness of the large mass cause internal restraint and buildup tensile stress within the material (Palomo *et al*. 1999). Tensile stress in the structure also depends upon the external restraint of the structural element. Time to crack depends not only on the tensile strength of the concrete but also on the tensile creep characteristics of the material (Duxon *et al*. 2007). One of the popular tests to determine the early-age-behavior of concrete under restrained shrinkage is the ring test (Moon and Weiss 2006). When the concrete ring deforms due to shrinkage the steel ring restrains the concrete which causes tensile stress in the specimen. In the ASTM C 1581 the ring provides a high degree of restraint while still allowing sufficient strain in the steel as the concrete shrinks (Ryan *et al*. 2010). Cracking in the ring specimen are assessed from the reading obtained from the strain gages attached to the inner surface of the steel ring. This method provides the strain data which can be converted with suitable mathematical equations to the stress developed in the concrete ring (See *et al*. 2003). An instrumented ring similar to the ASTM C1581 ring was evaluated in this study and used to obtain the restrained shrinkage behavior of six geopolymer concrete mixtures. Dimension of the ring specimens and thickness of the steel and concrete ring was selected according to the standard to follow the empirical equations already developed for stress calculation for restrained ring specimen (Jun *et al*. 2011). Testing and analysis procedure presented in this study illustrates how instrumented ring specimen can provide data on restrained stress and strain of geopolymer concrete. These results provide a basis for comparing the performance of different GPC mixtures under restrained shrinkage in the same environmental condition (Swayze 1942). This study deals with the result from shrinkage tests on the geopolymer concrete mix on both restrained and free shrinkage condition. Test was conducted to see the age of cracking and free shrinkage strain of geopolymer concrete. Data analysis was performed to evaluate the effect of various factors on the shrinkage behavior. Statistical analysis was conducted to establish the relationship between compressive strength at the age when shrinkage test was started and ultimate shrinkage strain. A theoretical model was emphasized and compared with existing empirical models to see the effectiveness of the best prediction equation for GPC.

Materials and mix design

Concrete mixtures were selected with different activator solution to fly ash ratio and for different target strength of the hardened concrete. Variables were selected to see the effect of activator solution to fly ash ratio on the shrinkage strain of geopolymer concrete. Compressive strength of the concrete varied in ranges between 25 MPa to 55 MPa. Samples were prepared without using any shrinkage reducing admixtures

(Guneyisi *et al*. 2010). Total amount of coarse and fine aggregate was constant for different mix design to see the effect of geopolymerization on the short and long term properties of GPC. All the mixes showed more than an 8 inch slump and the air content was below 4%. Concrete rings were kept on a vibrating table for 30 seconds to remove any entrapped air bubble inside it. A total of 6 different GPC and 1 ordinary portland cement (OPC) concrete mixture were evaluated. OPC mix was used as a control sample to monitor the shrinkage property from the testing and adjustment of the test setup.

Mix Proportion of Concrete

Concrete mixtures were selected from the specific strength range using the particular mix design of the activator solution and fly ash type. Strength of the concrete was controlled by the variation in activator solution to fly ash ratio (AS/FA). Class F fly ash was used for the design of concrete cylinders. Four different mix designs were produced by varying the AS/FA. Mix design was selected from the preliminary test. The detailed mix proportion for this group of specimens is presented in Table 1.

The second set of mix design was prepared to observe the effect of the extent of geopolymerization. In this test program, the aggregate to fly ash ratio was kept constant. Minimum compressive strength was attained using N silicate and 10M sodium hydroxide solution, and high strength was achieved using D silicate and 14M sodium hydroxide solution (Table 2). Activator solution to fly-ash ratio was 0.35 for both mix design.

A control mix of OPC to compare the results with the GPC was designed following the ACI guideline. OPC mix design was prepared to see the propagation of cracks and to use as a reference. Mix proportion was selected to get a hardened concrete with nominal strength of 55 MPa. Water cement ratio for this mix was 0.3.

Table 1. Mix design of GPC with the variation in AS/FA ratio.

Raw Material	Mix Design for different activator solution to fly ash ratio (kg/m^3)			
	0.35	0.45	0.55	0.65
NaOH (12M)	78.3	100.9	122.8	145.4
Silicate (N)	117.5	151.3	184.6	218.4
Fly Ash	559.6	559.6	559.6	559.6
River Sand	719.8	719.8	719.8	719.8
Pea Gravel	868.8	868.8	868.8	868.8

Table 2. Mix design of GPC with the variation in compressive strength.

Mix design for 25 MPa GPC (kg/m^3)		Mix design for 50 MPa GPC (kg/m^3)	
NaOH (10M)	78.3	NaOH (14M)	78.3
Silicate (N)	117.5	Silicate (D)	117.5
Fly Ash	597.5	Fly Ash	597.5
River Sand	612.4	River Sand	612.4
Pea Gravel	881.5	Pea Gravel	881.5

Table 3. Mix design of high strength OPC.

Working mix design in (kg/m^3)	
Cement (type-I)	692.5
Water	207.5
River sand	630.2
Pea gravel	868.5

The particular mix design in Table 3 was used to make a set of samples to find the strength gain over time and other mechanical properties. OPC samples were prepared and stored according to ASTM C31.

Test Method and Sample Preparation

The shrinkage test apparatus was prepared following ASTM C1581. The mold was prepared with a metal pipe section as the inner ring and a PVC two-part outer ring. Strain gages were attached to the inner surface of the metal ring to calculate the shrinkage strain caused by the drying of concrete. The data acquisition system was used to calculate the deformation occurred in the strain gage and the stress in concrete was also analyzed from this data. Ring specimens are more commonly used because of the benefits that those can easily be cast and the end effects are removed providing an axi-symmetric geometry (Kovler 1994). If the thickness of the steel is too large, deformation cannot be detected from the experiment. Such test setups provide qualitative evaluations, but do not establish a simple procedure to routinely quantify the restrained characteristics of the material (Grzbowski and Shah 1989). Strain at the inner surface of the steel ring is measured by the foil strain gage, which provides an accurate assessment of the time to crack. Cracking of the test specimens are indicated by a sudden decrease in compressive strain in the steel ring. The measured strain provides the basis for quantifying the restrained shrinkage behavior of the concrete specimen. Strain gages were placed at mid-height of the steel annulus, where the average strain is measured. Thickness of the

concrete wall was maintained at 1.5 inch for all specimens (Kwesi *et al*. 2014). The steel ring for the inner part of the mold was prepared from the steel pipe section of the standard size. The dimension of the steel ring was selected following ASTM C1581. Thickness of the steel ring was 0.5 inch and the inside diameter of the ring was 12 inch (30.48 cm). Steel pipe was cut according to the specified height 6 inch (150 cm) given in the standard. The edge of the ring was ground with fine sand paper. The inner and outer surfaces of the steel ring were cleaned using the sand blasting apparatus to remove any oil and grease. The rings made from the pipe section were further prepared to install the foil strain gage at the inner surface. Two strain gages were attached to the surface 180º apart. Data collection from the acquisition system was stopped when the crack formed at the outer surface of the concrete propagated to the inner ring, and there was no change in the reading obtained from the strain gages. The rate of shrinkage can change due to temperature and relative humidity. It is very important to keep concrete specimen inside a controlled environment to measure the shrinkage accurately. For this test an environment chamber with a dimension of 30ft x 15ft x 8ft was made with thick insulated aluminum wall.

The environmental control chamber kept the specimens at controlled temperature and humidity without too much stress on the mechanical devices. There was an arrangement to read the actual temperature and humidity by the digital panel from outside the chamber. For this experiment the environment chamber was kept at a constant temperature of 73±3º F and a relative humidity of 50±4% (Qiao *et al*. 2012).

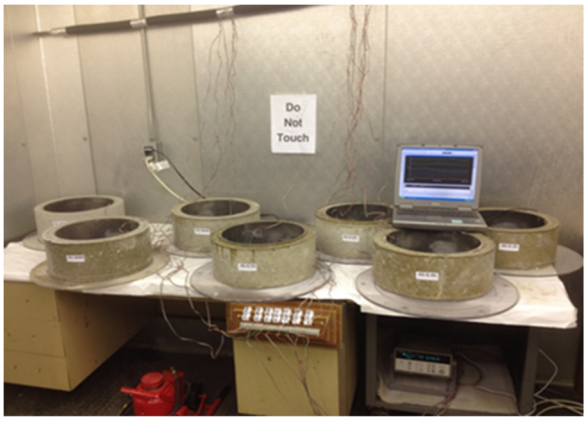

Figure 1. Test setup for strain measurement

Strain Data Calculation

Each sample was equipped with two strain gages. In order to record the strain for three months of testing, the data acquisition system is essential. Data logger used was manufactured by Hewlett Packard with 96 channels for strain readings. This arrangement allowed multiple data to be recorded at the same time. Every three days data was collected from the data logger to a computer. Data obtained from the data acquisition system was processed through the data logger software. Regular observations were made to see whether there is a trend of cracking in any of the ring specimen. Cracking strain capacity on the other hand was also determined by the elastic modulus test and splitting tensile strength test (Temuujin *et al*. 2009). Drying shrinkage strain was calculated considering the elastic and tensile creep strain in the concrete and balanced with the elastic contraction strain in the steel (Shah and Weiss 2006).

$$\varepsilon_{sh}(t) = \varepsilon_e(t) + \varepsilon_{cp}(t) + \varepsilon_{st}(t) \qquad (1)$$

Where $\varepsilon_{sh}(t)$ is the shrinkage strain, $\varepsilon_e(t)$ is elastic concrete strain, $\varepsilon_{cp}(t)$ is tensile creep strain and $\varepsilon_{st}(t)$ is the elastic steel strain at time t. Tensile stress in the concrete $\sigma_t(t)$ at time t is obtained from the following equation

$$\sigma_t(t) = \frac{E_{st} r_{ic} w_{st}}{r_{is} w_c} \varepsilon_{st}(t) \qquad (2)$$

Here E_{st} is the modulus of elasticity of steel. w_{st} and w_c are the wall thickness of the steel and concrete and r_{ic} and r_{is} are the internal radius of the concrete and steel respectively.

Theory

In 1982, the American Concrete Institute (ACI) recommended the procedure for the prediction of creep and shrinkage in its ACI-209R-82 code provisions (ACI 1982). The main inputs for shrinkage prediction are relative humidity, specimen size, curing period and age of loading. This model predicts the shrinkage strain. Correction factors are applied if the conditions are different from the ideal condition stated in the standard (Hardjito *et al*. 2004). This model can be applied to different kinds of concrete and is very simple to apply. The ACI-209R-82 code recommends the following expressions for shrinkage:

$$\varepsilon_{sh}(t, t_c) = \frac{t - t_c}{T_c + (t - t_c)} \varepsilon_{shu} \qquad (3)$$

According to CEB-FIP code proposed in 1990 and

is restricted to ordinary structural concrete. This model is based on the work of Muller and Hillsdorf (Hossain *et al*. 2003). The main input factors for the prediction of shrinkage are ultimate compressive strength, volume to surface ratio, age of curing, age of loading, and relative humidity. Unless special provisions are given, the model is valid for ordinary structural concrete having a compressive strength of 3000 psi (20 MPa) to 15000 psi (100 MPa), mean relative humidity 40-100% and mean temperature 5°C-30°C. Shrinkage strain was calculated from

$$\varepsilon_{sh}(t,t_c) = \left[160 + 10\beta_{sc}\left(9 - 0.1 f_{cm}\right)\right] \times 10^{-6}\beta_{RH}\sqrt{\frac{\{t - t_c\}}{\left\{350\left(\frac{2A_c}{100\mu}\right)^2 + (t - t_c)\right\}}} \quad (4)$$

B3 model as proposed by Bazant and Baweja (1995). It was developed at Northwestern University and is based on the statistical analysis of shrinkage data in a computerized data bank involving about 15,000 data points and about 100 test series. The latest B3 model considers more parameters than other prediction models (Bazant and Baweza 1995). The following parameters are used: a) relative humidity, b) exposure of concrete specimen to temperature prior to drying, c) size, d) cement type, e) coarse and fine aggregate, f) concrete density, g) concrete age, h) specimen ultimate strength. This model is predicted for w/c ratio of 0.30 to 0.85 and strength 2500 psi (17 MPa) to 10000 psi (65 MPa), a/c ratio 2.5-13.5 and cement content 160-720 kg/m^3. The mean shrinkage strain in the cross section is expressed as:

$$\varepsilon_{sh}(t,t_c) = -\varepsilon_{shu}\kappa_h S(t - t_c)$$

$$\varepsilon_{shu} = \alpha_1\alpha_2\left(0.091\, w^{2.1}\left[\left(f_{cm}\right)^{-0.28} + (270)\right]\right) \times \left(\frac{E_c(7 + 600\,t)}{E_c(t_c + \tau_{sh})}\right) \quad (5)$$

Sakata proposed this model for creep and shrinkage on concrete by a statistical method on the basis of experimental data. The equation can estimate the concrete creep and shrinkage strain (Sakata 1993). These prediction equations of shrinkage were adopted as the Japanese standard methods by the Japan Society of Civil Engineers (JSCE) in the revised standard Specification for Design of Construction and Concrete Structure published in 1996.

$$\varepsilon_{sht} = 0.177c + 121(w/c) - 16\log f'(t_0) - 31.4 \quad (6)$$

Gardner and Lockman (2001) proposed the GL 2000 model following the factors: a) relative humidity, b) average compressive strength, c) concrete member size, d) water to cement ratio, e) cement type, f) modulus of elasticity of concrete at the age of loading, g) concrete age at drying and h) concrete age at loading. This model is calibrated for compressive strength in the range of 2320 psi (16 MPa) to 11890 psi (80 MPa), with volume to surface ratio larger than 0.76, and w/c ratio between 0.40 to 0.60 (Gardner and Lockman 2001). The creep coefficient in this model is dependent on volume to surface ratio, age of drying, age of concrete at loading, and relative humidity. Following equations are used to calculate the creep compliance.

$$\varepsilon_{sh}(t,t_c) = \varepsilon_{shu}(1 - 1.18h^4) \times \sqrt{\left[\frac{t - t_c}{t - t_c + 0.15(V/S)^2}\right]} \quad (7)$$

Mix designs that survive longer without cracking are considered to perform better than those which crack earlier. The cracking area is also an indication of the performance of a mix. Some of the specimens which may crack early but have small cracks, and may not propagate toward the steel ring. Usually, the ring specimens start cracking from the outer surface near either the top or the bottom, and then the crack continues to move inward toward the ring over time (Bentz *et al*. 1995). The speed at which the crack propagates toward the steel ring depends on the mix design. It is possible that the crack does not propagate fully towards the ring. When the crack reaches the ring, it causes a release of compressive stress upon the steel ring. Shrinkage strain values for different mix designs were calculated using the empirical equations and test data obtained from the data acquisition system were compared. In this study ACI, Bazant B3, CEB, GL2000, and Sakata models were evaluated on their effectiveness and accuracy in predicting the shrinkage strain of the different GPC mixes. Tensile creep parameters and restrained shrinkage strain calculation was performed using the free shrinkage strain, steel ring stain, modulus of elasticity and flexural tensile strength of GPC. Empirical equations given in ACI 209 were used to calculate the predicted strain at time t. Given the elastic

strain at cracking, an analysis based on free shrinkage strain alone without considering the tensile creep will give cracking of the concrete much earlier than the actual cracking days. Thus, the tensile creep significantly increased the time to cracking of all concrete mixtures. As expected the lower activator solution to fly ash ratio for GPC mixtures yield longer times to cracking (Jensen and Hansen 2001). This difference is explained by considering the magnitude of tensile creep effect on the cracking resistance. The larger magnitude of tensile creep coefficient of high strength low activator solution to fly ash ratio mixtures also corresponds to the longer days to cracking. This result is also linked to the higher geopolymeric reaction in high strength GPC. The tensile creep coefficients under restrained shrinkage are smaller than the coefficient under free shrinkage and fixed stress (Zuanfeng *et al.* 2011). A lower tensile creep under a state of increasing stress occurs when the specimen is restrained.

Results and Discussion

The cracking behavior of a particular mix is very much dependent upon the liquid content of the mix. The environmental factors such as humidity and temperature that changes the shrinkage behavior were kept constant for all samples so the evaporation effect was neglected. In this study, one of the reason behind the early age cracking was found to be the liquid content of the concrete mix. Non-structural causes were: plastic shrinkage, thermal deformation and autogenous shrinkage. Plastic shrinkage occurs because of differential settlement and excessive evaporation of water from the concrete surface. Thermal shrinkage is largely due to considerable heat generated from the chemical reaction. Autogenous shrinkage is caused due to reduction of volume and self-desiccation of internal pores. Free shrinkage test results were obtained from the prism specimen using the length comparator. The results obtained from the test are shown in Figure 2. Among the models used to predict the free shrinkage of the concrete, the Sakata model was very close to the experimental data observed for various GPC samples. From the test results, it was observed that the water content has a significant effect on the drying shrinkage of the GPC. For a mix design with 0.35 AS/FA ratio, it took 86 days and with 0.65 AS/FA ratio, the concrete ring was cracked in only 42 days. GPC with higher strength took more time to form the surface crack. The high strength of the GPC prevents the tensile crack formation. Test result obtained from 4000 psi and 8000

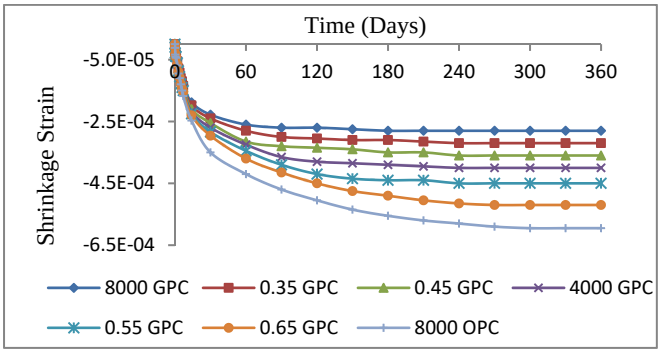

Figure 2. Free shrinkage strain.

psi GPC reflect the hypothesis that geopolymer with high strength has less drying shrinkage than that with lower compressive strength and lower polymerization reaction. Test result obtained from this study puts forth a table with this coefficient for the shrinkage measurement of the GPC with a different activator solution to fly ash ratio. The sand to aggregate ratio had little effect on the mechanical properties or the cracking potential of the mixes.

From compressive strength test results, it was found that OPC had 28 days strength of 55 MPa. GPC sample designed for this similar strength acquired this after 24 hours of heat curing. Figure 2 shows that the first two weeks strain rate is steep for all specimens while there is a change in strain rate at the end of two weeks. After 120 days GPC sample with different AS/FA ratio reached a steady state. At the end of one-year strain in the OPC sample is 200% more than the strain in the GPC sample having the same liquid content at the beginning (35%). The reason behind this can be associated with the formation of a dense polymer matrix that leaves little space for shrinkage in GPC. It can be observed from the graph that the maximum strain from the GPC sample was more than 500 micro strain (for 0.65 AS/FA) and the minimum was around 200 micro strain (for 0.35 AS/FA). This is important data to use in combination with the total strain to find the basic shrinkage for the corresponding mix design of the GPC.

A characteristic comparison plot is shown in Figure 3. All control data are available upon request. It can be observed that ACI model overestimated the shrinkage strain. Strain obtained from the SAKATA model successfully predicted and was very close to the experimental data. Same phenomena were observed for the other samples with different activator solution to fly-ash ratio. This is why the SAKATA model is recommended to predict the shrinkage strain of GPC.

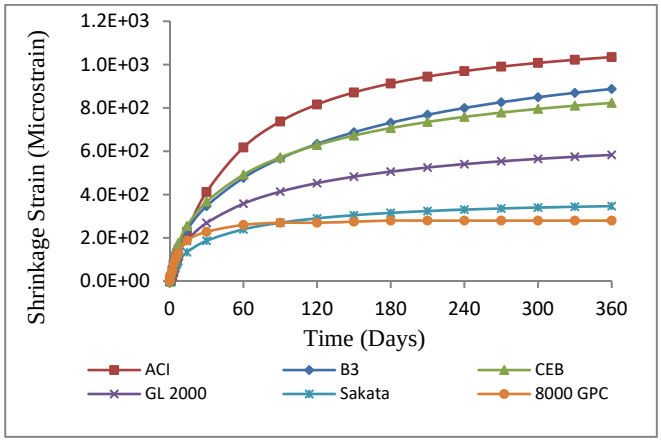

Figure 3. Empirical and experimental data plot

Conclusion

In this paper free and restrained shrinkage of geopolymer concrete was measured at a constant temperature and humidity. The effect of activator solution to fly ash ratio and final compressive strength of GPC was observed on the shrinkage behavior over time. It has been observed that the free shrinkage strain of GPC is less than the data predicted by the empirical equation most of the cases. Each of the mixes had an elastic modulus in the range of about 5000 Ksi (34 GPa) and a tensile strength in the range of 650 Psi (4.5 MPa). Every mix in the AS/FA group cracked around 90 days or stopped putting any compression on the inner ring. The free shrinkage at day 90 for each mix was in the range of 350 to 450 micro strain. Tensile stress generated by restrained shrinkage of the concrete are significant in the first week after casting and lead to a fracture of the material. The role of the tensile creep in the relaxing shrinkage stress is substantial and reduces the stress. The SAKATA model had the closest agreement with the experimental data. The overall comparison with the available models showed the proposed model in this study has the closest correlation with the experimental data.

Acknowledgements

The author would like to thank Trenchless Technology Center of Louisiana Tech University for the use of its facilities. Special thanks to Dr. Carlos Montes for his suggestions and help to access the material characterization lab of the micro-manufacturing institute of Louisiana Tech University.

Literature Cited

Bazant ZP and **S Baweza.** 1995. Justification and refinements of model b3 for concrete creep and shrinkage1statics and sensitivity. Materials and Structure 28:415-30.

Bentz DP, DA Quenard, VB Bouny, and **HM Jennings.** 1995. Modeling drying shrinkage of cement paste and mortar part1. Structural models from nanometers to millimeters. Materials and Science 28:450-58.

Bernal JD, Dasgupta DR, and **Mackay AL.** 1959. The oxides and hydroxides of iron and their structural inter-relationships. Clay Materials Bulletin 21:15-30.

Duxon PA, J Fernandez, JL Provis, GC Lukely, A Palomo, and **JS Van Deventer.** 2007. Geopolymer technology: the current state of the art. Journal of Materials Science 142:2917-33.

Gardner NJ, and **MJ Lockman.** 2001**.** Design provisions for drying shrinkage and creep of normal-strength concrete. ACI Materials Journal 98:159-67.

Grzbowski M and **SP Shah.** 1989. Model to predict cracking in fiber reinforced concrete due to restrained shrinkage. Magazine of Concrete Research 41:125-35.

Guneyisi E, M Gesoglu, and **E Ozbay.** 2010. Strength and drying shrinkage properties of self-compacting concretes incorporating multi-system blended mineral admixtures. Construction and Building Materials 24:1878-87.

Hardjito D, SE Wallah, DM Sumajouw, and **BV Rangan.** 2004. On the development of fly ash-based geopolymer concrete. ACI Materials Journal 101:467-72.

Hossain AB, B Pease, and **J Weiss.** 2003. Quantifying early-age stress development and cracking in low water to cement concrete: restrained ring-test with acoustic emission. Transportation Research 1834:24-32.

Jensen OM and **PF Hansen.** 2001. Water-entrained cement based materials I, principle and theoretical background. Cement and Concrete Research 31:647-54.

Jun Z, H Dongwei, and **C Haoyu.** 2011. Experimental and theoretical studies on autogenous shrinkage of concrete at early ages. Journal of Materials in Civil Engineering 23:312-20.

Kovler K. 1994. Testing system for determining the mechanical behavior of early age concrete under restrained & free uniaxial shrinkage. Materials and Structures 27:324-30.

Kwesi SC, B Trevor, and **T Alan.** 2014. Drying shrinkage and creep performance of geopolymer concrete. Journal of Sustainable Cement Based Materials 2:35-42.

Moon JH and **J Weiss.** 2006. Estimating residual stress in the restrained ring under circumferential drying. Cement and Concrete Composites 28:486-96.

Palomo A, MW Grutzeck, and **MT Blancon.** 1999. Alkali-activated fly ashes A cement for the future. Cement and Concrete Research 29:1323-29.

Qiao Z, J Linhua, and **J Xu.** 2012. Models for autogenous shrinkage in low water- binder ratios concrete. Advanced Materials Research 487:435-39.

Ryan H, B Peter, B Dale, N Tommy, and **W Jason.** 2010. Plastic shrinkage cracking in internally cured mixtures made with pre-wetted light weight aggregate. Concrete International 32:49-54.

Sakata K. 1993. A study of moisture diffusion in drying and drying shrinkage of concrete. Cement and Concrete Research 13:216-24.

See HT, EK Attiogbe, and **Miltenberger MA.** 2003. Shrinkage cracking characteristics of concrete using ring specimens. ACI Materials Journal 100:239-45.

Shah HR,and **J Weiss.** 2006. Quantifying shrinkage cracking in fiber reinforced concrete using the ring test. Materials and Structure 39:887-99.

Swayze MA. 1942. Early concrete volume changes and their control. ACI Journal. 38:145-151.

Temuujin JA, A Van Riessen, and **R Williams.** 2009. Influence of calcium compounds on the mechanical properties of fly ash geopolymer pastes. Journal of Hazardous Materials 167:82–88.

Zuanfeng P, CF Chung, and **Y Jiang.** 2011. Uncertainty analysis of creep and shrinkage effects in long-span continuous rigid frame of Sutong Bridge. Journal of Bridge Engineering 16:248-58.